

Eight-coordinate fluoride in a silicate double-four-ring

Maarten G. Goesten^{a,1}, Roald Hoffmann^{b,1}, F. Matthias Bickelhaupt^{c,d}, and Emiel J. M. Hensen^a

^aInorganic Materials Chemistry, Schuit Institute of Catalysis, Eindhoven University of Technology, 5600 MB Eindhoven, The Netherlands; ^bDepartment of Chemistry and Chemical Biology, Baker Laboratory, Cornell University, Ithaca, NY 14853-1301; ^cDepartment of Theoretical Chemistry, Vrije Universiteit Amsterdam, 1081 HV Amsterdam, The Netherlands; and ^dInstitute of Molecules and Materials, Radboud University Nijmegen, 6525 AJ Nijmegen, The Netherlands

Contributed by Roald Hoffmann, December 16, 2016 (sent for review September 21, 2016; reviewed by Kelling Donald and Lars Kloo)

Fluoride, nature's smallest anion, is capable of covalently coordinating to eight silicon atoms. The setting is a simple and common motif in zeolite chemistry: the box-shaped silicate double-four-ring (D4R). Fluoride seeks its center. It is the strain of box deformation that keeps fluoride in the middle of the box, and freezes what would be a transition state in its absence. Hypervalent bonding ensues. Fluoride's compactness works to its advantage in stabilizing the cage; chloride, bromide, and iodide do not bring about stabilization due to greater steric repulsion with the box frame. The combination of strain and hypervalent bonding, and the way they work in concert to yield this unusual case of multiple hypervalence, has potential for extension to a broader range of solid-state compounds.

chemical bonding | main-group chemistry | hypervalence | zeolite chemistry

What is the maximum number of atoms to which a main-group element may bond? Four, one would normally think. But, hypervalence and delocalized bonding enlarge the upper range—no one bats an eyelid at silicon binding 6 ligands, and there exist cases of arguably 10-coordinate Si (1, 2). Much thinking on high coordination focuses on atomic or ionic radii, and packing considerations. Or, one can approach the problem from a quantum-chemical perspective. In this paper, we follow the latter course, and operate at the crossing point between molecular and extended systems. We explore how the upper bound for coordination number is determined by attractive and repulsive forces, adding in a factor of strain, associated with deforming a molecular cage that entraps an element in its center.

The stage for this work is set by a simple and common motif in catalysis and separation: the silicate double-four-ring (D4R), one of the archetypal building blocks in large-pore zeolites. By use of relativistic density-functional theory (DFT) calculations and Kohn–Sham molecular orbital theory (3–6), we will see that within this box-like environment, fluoride coordinates, actually binds, to eight silicon atoms.

Discussion

Halides in the Molecular D4R Cage. In zeolite synthesis, the use of fluoride has led to the discovery of new, silica-rich zeolite topologies (7), and has further been used to remove lattice defects through synthetic and postsynthetic procedures. It is notable that F[−] exchange is reversible by alkaline treatment, with a single exception—when F[−] is located in framework-incorporated D4R units, where the anion is tightly bound, in fact irremovable (8). Other halides are not known to enter this small box. Crystallography has shown that fluoride resides in the center of the D4R box (9), in contrast to double-five-ring and double-six-ring units, other common zeolitic building blocks, where fluoride binds to a hypervalent silicon atom in a cage corner (10, 11).

The interaction of D4R with fluoride has not escaped the attention of theoreticians. George and Catlow calculated significant charge transfer (based on a Mulliken population analysis) for the insertion of fluoride in D4R, and a binding energy of just under 100 kcal/mol (12, 13). A thorough survey by Hagelberg

and coworkers (14) of a variety of halide and other insertion compounds in a D4R model with external hydrogens also indicated a substantial binding energy for fluoride (71 kcal/mol), further supported by a study by Tossell (15). Charge polarization rather than bonding was thought to be the responsible factor. These calculations also considered exohedral complexes, and indicated that inclusion proceeds through a transition state that leaves the cage intact. The calculated shape of D4R's lowest unoccupied molecular orbital (LUMO), provided in an extensive review by Laine and Roll, is thought-provoking (16). It appears highly delocalized, and is centered in the cage.

Let us commence with a stepwise analysis of fluoride's position in D4R, and probe what happens when it is moved off-center (we will refer to D4R with fluoride inside as F[−]@D4R). In our calculations, we used the single-entity, silsesquioxane D4R. We chose hydroxyl groups to terminate the Si vertices, pointing out and bent at O (17). This molecular box is shown in two views in Fig. 1. DFT calculations carried out at ZORA-BP86-D3(BJ)/QZ4P indicate that the most stable geometrical conformation has the D4R box in slightly distorted *D*_{2d} symmetry, 0.8 kcal/mol down in energy from strictly *D*_{2d}. The geometry of the box frame, i.e., the Si vertices and O edges, is in almost perfect agreement with the experimental structure from Auf der Heyde et al. (18). The lower level of symmetry, with respect to *T*_h and *O*_h, results from the angled attachment of hydroxide ligands to the vertices of the box. Further consideration of symmetry will come later.

Now taking this box, and moving fluoride, chloride, bromide, and iodide along a diagonal, with displacement from center *s*, we found the preferred location for all anions to be at the very center, which is in line with the experimental results for fluoride in zeolites, and consistent with the aforementioned theoretical work. This is graphically depicted in Fig. 2, in which the black

Significance

Although strain and bonding are often antagonists in chemistry, they may also work together. When fluoride enters a silicate double-four-ring (D4R), their conjoined effect leads to fluoride binding to 8 silicon atoms. The strain comes from D4R, a molecular unit that acts (and looks) like a box. And, as we can expect from that geometrical constraint, it experiences strain when being deformed. Avoiding such deformation, the box pushes fluoride toward its center. Yet even there, fluoride engages in orbital overlap (hypervalent bonding) with the highly delocalized antibonding orbitals of D4R, and significant charge transfer occurs. The unusual number of bonds, around the smallest existing anion, leaves us pondering the limits of hypervalence.

Author contributions: M.G.G., R.H., F.M.B., and E.J.M.H. designed research; M.G.G. and R.H. performed research; M.G.G., R.H., and F.M.B. contributed new reagents/analytic tools; M.G.G., R.H., and F.M.B. analyzed data; and M.G.G. and R.H. wrote the paper.

Reviewers: K.D., University of Richmond; and L.K., KTH Royal Institute of Technology.

The authors declare no conflict of interest.

¹To whom correspondence may be addressed. Email: M.G.Goesten@TUE.NL or rh34@cornell.edu.

This article contains supporting information online at www.pnas.org/lookup/suppl/doi:10.1073/pnas.1615742114/-DCSupplemental.

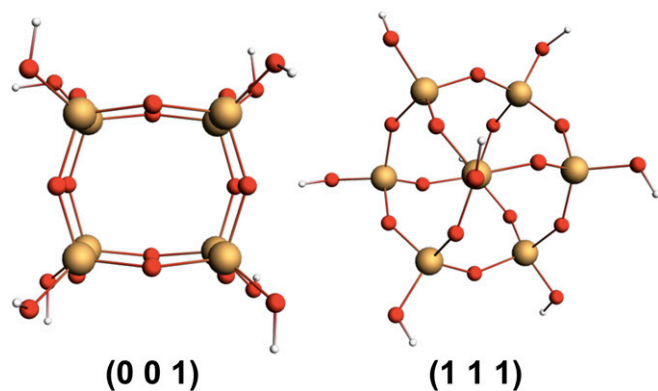


Fig. 1. Silsesquioxane D4R as used in our calculations. The figure shows views along the (001) and (111) directions.

line acts as a common energy zero reference, representing the energies of D4R and the halide anions at an infinite distance. The difference between fluoride and its congeners is striking: only fluoride is stabilized. The potential energy surface (PES) for moving fluoride across the cage contains a plateau around the very center of the cage, at about -80 kcal/mol. Fitting the curve to a sixth-degree polynomial revealed significant contribution of both fourth- and sixth-order anharmonicities to a quadratic potential, approaching the form $ax^2 + b(x^4 + x^6)$. If the cage is frozen in geometry upon diagonal movement of fluoride, the resulting potential is parabolic (Fig. 3), so the complexity of the real PES arises from the cage's deformation to stabilize conformations where fluoride is off the cage center.

We have also studied the possibility of exohedral bonding of fluoride. The results are discussed in the *SI Appendix*; such

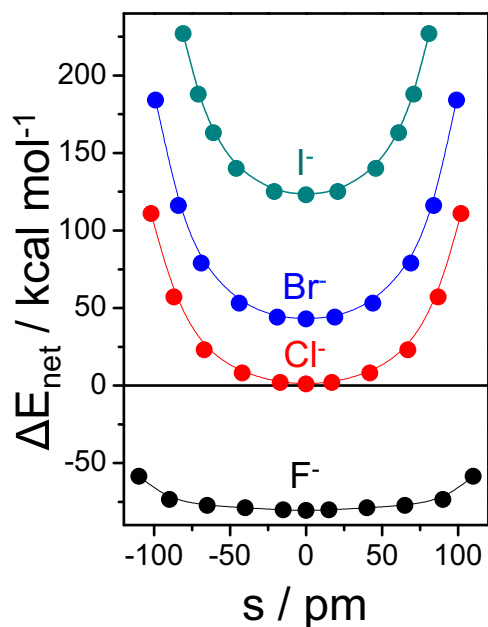


Fig. 2. Energetics of a linear transit of fluoride, chloride, bromide, and iodide along a cage-diagonal path of 11 points. s is the distance from the center. The relative energies of the corresponding geometrically optimized structures are plotted relative to an energy zero of the halide anion and D4R at an infinite distance, calculated at ZORA-BP86-D3(BJ)/QZ4P. The distance from the center of the box to a Si atom is 268 pm.

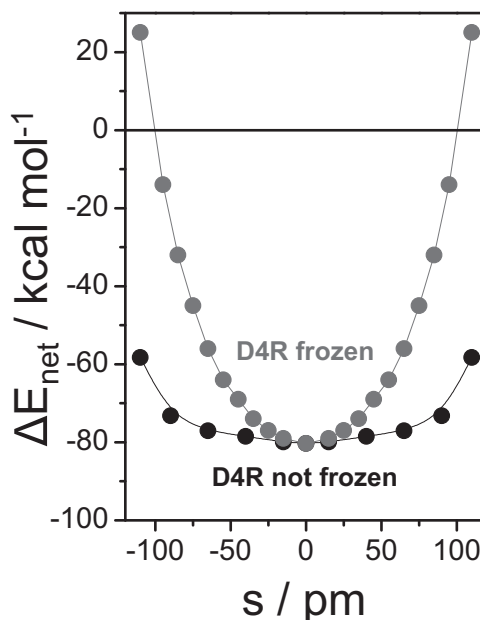


Fig. 3. Linear transit of fluoride, analogous to that in Fig. 2, but with the D4R fragment frozen in geometry (gray curve). s is the distance from the center of the box.

bonding is strong (less than 0.2 kcal/mol up from fluoride in D4R's center), and hypervalent at one Si of the cage.

D4R cages are not the only strong fluoride binders in chemistry (19, 20). Of particular interest to us is a burgeoning field of ingeniously designed, supramolecular fluoride receptors (21–25). The binding energies of these are just as large, and sometimes larger than that of the D4R box. Bonding in these fluoride sequestering agents is accomplished through strong hydrogen bonds. We think there is a strong hypervalent bonding component in these systems as well, involving charge transfer.

To summarize what we have found to this point: The experimentally known strong binding of fluoride, and specifically that halide ion, is checked by our calculations. These are also in general agreement with those previously made by Hagelberg and coworkers for the halide series. We proceed to reason out why this is so—why fluoride, whence the unusual plateau?

The Nature of the Interaction. Solid-state ^{19}F NMR experiments reveal a highly downfield-shifted resonance for fluoride in D4R, inferring a large degree of charge transfer from the central element to the box (26). Could covalence (here meant in the general sense of both covalent and polar, donor–acceptor bonding), rather than simple Coulomb forces, play an important role, as well as in shaping the unusual potential energy curve for fluoride moving in the box? And, why is it only fluoride that is dramatically stabilized in the central region of the box?

Let us attempt to unravel the halide–cage interaction using an energy decomposition analysis (EDA) (6). We will from now on refer to the halide anion–D4R interaction as $\text{X}^-@D4R$ (with $\text{X} = \text{F}, \text{Cl}, \text{Br}, \text{I}$). In EDA, the interaction is decomposed into three terms: at first, we have the electrostatic term, ΔE_{elstat} , which we expect to be dominated by Coulombic stabilization between the negatively charged electron density of X^- and the positively charged silicons of D4R (and vice versa). Second is the non-classical Pauli or exchange repulsion, between electrons possessing parallel spins (6). As bond formation between X^- and D4R will increase the number of electrons of parallel spin, the associated term ΔE_{Pauli} is repulsive. Finally, we consider the stabilizing orbital interactions, ΔE_{oi} , involving the mixing and

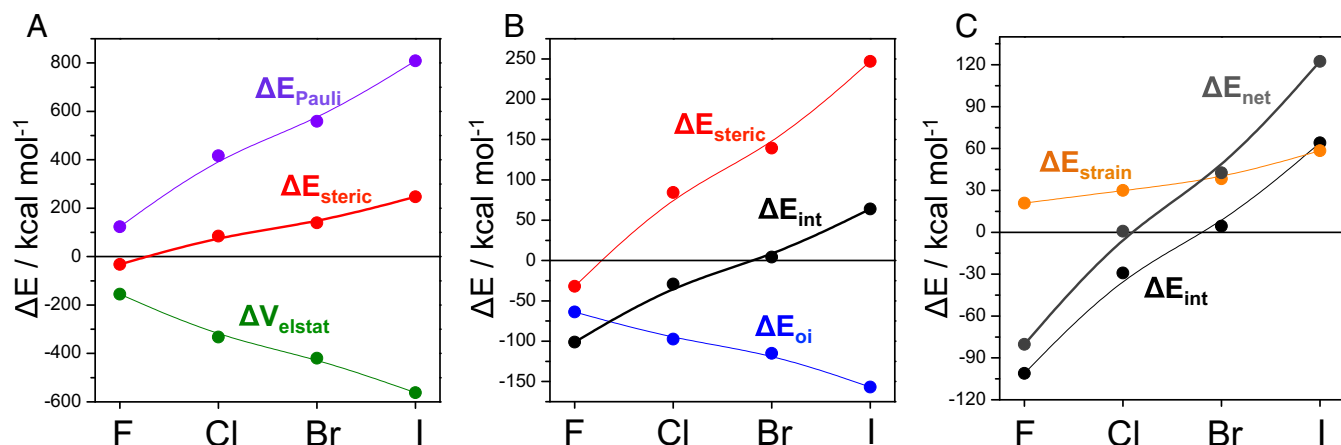


Fig. 4. (A) EDA of all halide–cage interactions at ZORA-BP86-D3(BJ)/QZ4P, with ΔE_{steric} established as $\Delta V_{elstat} + \Delta E_{Pauli}$. (B) ΔE_{int} decomposed in terms of ΔE_{steric} and ΔE_{oi} . (C) ΔE_{net} established by adding ΔE_{strain} to ΔE_{int} .

charge transfer between the orbitals of X^- and those of the box. This is the third term in the total interaction energy expression, which we associate with covalence (broadly speaking, and including polar bonding). It is roughly proportional to $(S^{A|X})^2$, the orbital overlap between the interacting orbitals of A and X squared (27).

We calculate ΔV_{elstat} , ΔE_{Pauli} , and ΔE_{oi} for $X^-@D4R$, as well as a correction for dispersion, ΔE_{disp} , obtained from the empirical Grimme formulation (28). This last term turned out to be comparatively small for all cases, and we refer to the *SI Appendix* for its numeric values. In general, ΔV_{elstat} is large and negative and ΔE_{Pauli} is large and positive. As first suggested by Ziegler and Rauk (29), we combine the terms for electrostatic interaction and Pauli repulsion into a term for steric interaction, $\Delta E_{steric} = \Delta V_{elstat} + \Delta E_{Pauli}$. This term gages the overall energy change associated with the mixing of electronic densities of the halide anion and D4R, without charge transfer taking place. In this manner, the role of stabilizing orbital contributions to bonding is brought to the fore.

Fig. 4A displays the (de)composition of ΔE_{steric} for all halide anions. The Pauli repulsion rises more steeply than the fall of the electrostatic term, leading to a ΔE_{steric} that is negative only for fluoride, and increasingly positive for the other halides. Fig. 4B decomposes the net $X^-@D4R$ interaction, ΔE_{int} , in terms of the steric term ΔE_{steric} and orbital interaction ΔE_{oi} . It is clear that orbital interaction plays a significant role in the binding of $F^-@D4R$: ΔE_{oi} amounts to 66% of the total interaction ($\Delta E_{oi} + \Delta E_{steric}$) at the quadruple- ζ (QZ4P) level. The use of even-tempered basis sets containing more diffuse functions, ET-pVQZ and ET-QZ3P-1DIFFUSE, leads to effectively identical estimates (*SI Appendix*). For the larger halides, with their increasing radius, the orbital stabilization ΔE_{oi} (even if growing in magnitude) is increasingly overtaken and nullified by the steric term (which, as we saw, is dominated by Pauli repulsion). The net change in energy relative to separate halide and D4R, ΔE_{net} , which was plotted in Fig. 2, differs from the instantaneous interaction ΔE_{int} as defined above, by ΔE_{strain} . This is the energy needed to deform the box to adjust to the halide bonding (30). These terms are plotted in Fig. 4C; it is now clear why, within this interplay of chemical interaction and molecular deformation, only $F^-@D4R$ is stabilizing (yet $Cl^-@D4R$ comes close).

We move back to the PES curves in Fig. 1. The gray curve in Fig. 3 is a surface for ΔE_{int} with a frozen D4R fragment. If we now decompose the real PES of $F^-@D4R$ into two surfaces, one for ΔE_{strain} and one for ΔE_{int} , we see that the former is of parabolic shape, and the latter contains the fourth- and sixth-order

anharmonicities that we obtained before (Fig. 5). This was confirmed by fitting the separate curves (*SI Appendix, Fig. S1*).

Thus, in allowing D4R to deform, the surface of ΔE_{int} transforms from harmonic and box-centered to anharmonic and stabilized nearer the walls. In fact, as fluoride moves closer to the corner, the cage, under increasing strain, pushes its vertices toward the typical trigonal bipyramid geometry for pentacoordinate, hypervalent Si: in this case, three equatorial bonding Os and a HO–Si–F axis. *SI Appendix, Fig. S5* shows the geometry in detail.

The deformation strain of D4R's framework clearly plays a role in the bonding we analyze. Let us test our understanding: If we conjecture that the PES of moving an element/ion across the D4R cage can be understood as consisting of a PES for strain as well as interaction, we should be able to predict what happens when either strain, or interaction, is dominant. For example, the diagonal movement of a species which engages in no or little interaction should give rise to a parabolic PES which barely differs from that for strain (Figs. 3 and 5). This is indeed confirmed

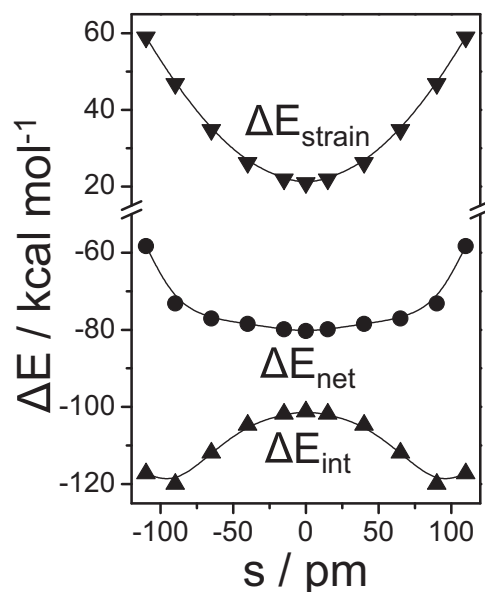


Fig. 5. Decomposition of fluoride's PES (Fig. 2) into terms of ΔE_{strain} and ΔE_{int} . s is the distance from the center of the box.

Fig. 7 summarizes the dominant interactions in terms of an MO diagram with the computed orbitals. These interactions underline the combination of delocalization and symmetry in D4R's accepting orbitals, which give rise to our set of donor-acceptor interactions.

Can we measure the extent of bonding between the fluoride and the silicons at cage vertices? Examination of the MO coefficients clearly indicates bonding F–Si combinations. Fully aware of the ambiguity of various bond indices, we do find 8 Si–F Mayer (33) bond indices of 0.11 each. The F–O bond indices are virtually zero (about -0.005). We conclude that in this box we have eight-coordinate fluoride, taking part in eight hypervalent interactions with the Si's at the box vertices.

Confinement, Strain, Molecules, and Solids. In a way, the scenario of this work upends earlier criteria for the viability of hypervalence, by Braïda and Hiberty (34, 35) and Braïda et al. (36) within valence-bond theory (34–36) and by Bickelhaupt and coworkers within MO theory (37). These models relate increasing viability of hypervalence to decreasing ionization potential and increasing atomic radius of the central element. In the present work it is observed, and rationalized, that an increasing ionization potential and decreasing (ionic) size make for better binding in the center, i.e., $F^- > Cl^- > Br^- > I^-$. This swap of trends is a consequence of D4R acting as a ligand box, in the sense that the eight Si's would not find themselves in the relative proximity of just over 300 pm, if not interattached. We verified this with a geometry optimization on eight $Si(OH)_4$ and eight SiF_4 molecules.

The geometry (and viability) of “ordinary” hypervalence in molecules is in the first instance controlled by the central element, secondarily by the electronegativity of the ligands. For instance, Si can bind five atoms in a trigonal bipyramid in $[SiH_3F_2]^-$, whereas C would stay tetrahedral, i.e., CH_3F with a F^- (27). In the case of $F^-@D4R$, it is the other way around. The presence of a rigid geometry, the D4R box, controls whether a central element would fit. Mainly determined by Pauli repulsion (Fig. 4), this may be referred to as an effect of confinement. The hypervalent bonding between fluoride and the eight surrounding Si's then adds a strong (hypervalent) bonding component.

This brings us to an interesting perspective, because the glue holding the eight Si's together, in this case strong Si–O bonds, makes a connection to extended systems. In many of these systems, high coordination numbers are the result of packing forces, although they may also arise from metallic bonding interactions. The barrier that packed structures experience upon lattice deformation, required to dislodge a single atom from its position, bears analogy to the strain of deformation that holds fluoride in D4R's center. If, in the resulting enforced confinement, there is

Table 2. Separate-symmetry contributions to ΔE_{oi} of the F–D4R interaction

Symmetry	$\Delta E/kcal\ mol^{-1}$
a_{1g}	–9.9
a_{2g}	–0.2
e_g	–2.4 (–1.2)
t_{1g}	–2.0 (–0.7)
t_{2g}	–5.1 (–1.7)
a_{2u}	–0.7
a_{1u}	0.0
e_u	–0.8 (0.4)
t_{1u}	–39.7 (–13.2)
t_{2u}	–3.0 (–1.0)

Values in brackets denote the single-orbital contribution for the doubly- and triply degenerate symmetries.

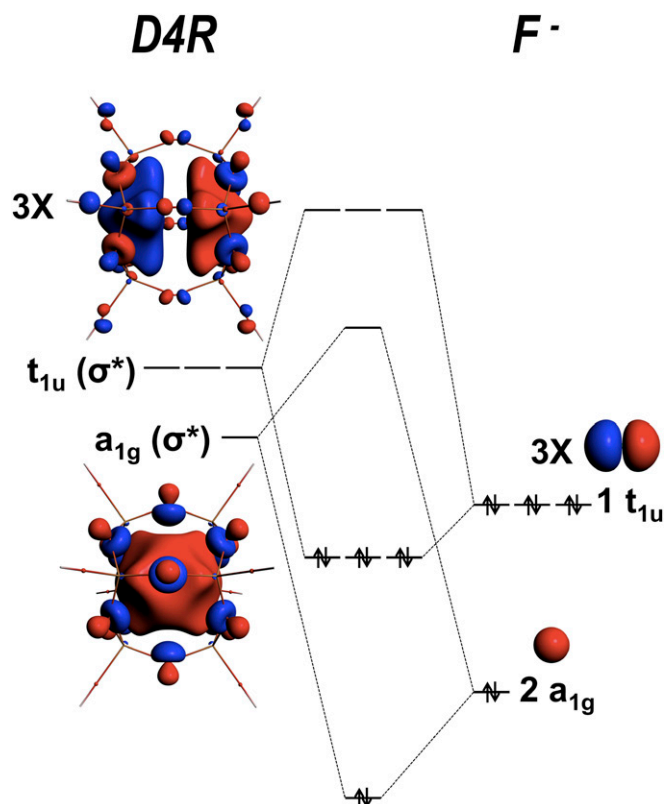


Fig. 7. Computed σ^* -orbitals of a_{1g} and t_{1u} symmetry and their interaction with fluoride's a_{1g} and t_{1u} orbitals.

also a possibility of covalent or dative bonding, commensurate high coordination, real bonding and not just packing, ensue.

Even as we make the analogy, we are aware that there is something delicate about $F^-@D4R$. The strain D4R experiences upon moving the fluoride off-center is small compared with any lattice deformation in an extended structure, and in fact, just overcomes the additional stabilization associated with a shorter, stronger Si–F bond (we refer back to Fig. 5).^{*} It would take only a small, persistent push to have the structure overcome strain, and deform toward increased Si–F interaction, as we would expect for a discrete molecule.

In exploring the fine interplay between interaction and strain, we intend to consider the feasibility of 12-fold coordination in hexagonal or face-centered close-packed analogs. We think strain and hypervalence work together in these systems as well. Analyzing them will require us to plunge into a gray zone between molecular and solid-state chemistry, which is actually where we want to be.

The strain–bonding relationship we propose occurs elsewhere in chemistry too. $F^-@D4R$ reminded us of the remarkable story that Shaik and Hiberty unfolded to us for benzene—the π -electron system of the molecule would like to distort, even if there is a stabilizing aromatic interaction. The σ -system resists, keeps the molecule D_{6h} , and allows the orbital stabilization to show itself (38).

Indeed, strain and bonding need not be opposed; they may act in concord.

^{*}Naturally, the strain PES will be considerably more steep were D4R embedded in a zeolite lattice. The effect of zeolite topology on this strain factor remains to be examined.

An Epilogue: A Few Comments on Experimental Chemistry. Clearly some zeolite topologies containing D4R units require fluoride addition in synthesis (39). The earlier papers of George and Catlow (12, 13), Hagelberg and coworkers (14), Tossell (15), and Laine and Roll (16), and our analysis show the magnitude and nature of the bonding. Fluoride acting as a template is similar to that of a stabilizing ligand, providing net stabilization of more than 80 kcal/mol for a single D4R unit, as calculated here. In addition, our orbital analysis sheds light on the fascinating chemistry we may find in all-silica zeolites. Current models of adsorption and separation by all-silica zeolites rely on a classical picture, with kinetic diameters and pore mouths as sole factors in directing performance. We have shown that there is an additional, coordination-chemical dimension to all-silica zeolites as well, with highly delocalized bonding a factor.

A question remains. Could other molecules enter this archetypal zeolite cage? The room inside is small. The hypervalent

bonding potential of the central site that we identified would point to anions or more electronegative atoms. We estimated that hydride ($\Delta E_{net} = -63$ kcal/mol), the lithium cation [$\Delta E_{net} = -35$ kcal/mol, in line with a result computed by Hagelberg and coworkers (14)], and hydroxide ($\Delta E_{net} = -67$ kcal/mol) engage in significant interaction with D4R as well. But, exploitation of D4R's remarkable properties would require removal of fluoride from the as-synthesized all-silica zeolite, a challenge not yet met. Some very recent synthetic explorations make this possibility seem not so far away (40, 41). We hope this work will further spur such searches. One is also impelled to think about using the hypervalent bonding propensities of fluoride to stabilize other polyhedral cages, formed of transition metals as well as group 14 elements.

ACKNOWLEDGMENTS. R.H. is grateful to the National Science Foundation for the support of this work through Research Grant CHE-1305872.

1. Wells AF (1984) *Structural Inorganic Chemistry* (Oxford Univ Press, Oxford), 5th Ed, pp 987–991.
2. Jutzi P, Holtmann U, Bögge H, Müller A (1988) Protonation of decamethylsilicocene. *J Chem Soc Chem Commun* 1988(4):305–306.
3. Bickelhaupt FM, Nibbering NMM, Van Wezenbeek EM, Baerends EJ (1992) Central bond in the three CN• dimers NC-CN, CN-CN, and CN-NC: Electron pair bonding and Pauli repulsion effects. *J Phys Chem* 96(12):4864–4873.
4. SCM (2016) ADF Modeling Suite. Available at <https://www.scm.com/adf-modeling-suite/>. Accessed January 7, 2017.
5. Velde Te G, et al. (2001) Chemistry with ADF. *J Comput Chem* 22(9):931–967.
6. Bickelhaupt FM, Baerends EJ (2000) *Kohn-Sham Density Functional Theory: Predicting and Understanding Chemistry* (Wiley, New York).
7. Cundy CS, Cox PA (2003) The hydrothermal synthesis of zeolites: History and development from the earliest days to the present time. *Chem Rev* 103(3):663–702.
8. Liu X, Ravon U, Tuel A (2011) Evidence for F/SiO⁻ anion exchange in the framework of As-synthesized all-silica zeolites. *Angew Chem Int Ed Engl* 50(26):5900–5903.
9. Corma A, Puche M, Rey F, Sankar G, Teat SJ (2003) A zeolite structure (ITQ-13) with three sets of medium-pore crossing channels formed by 9- and 10-rings. *Angew Chem Int Ed Engl* 42(10):1156–1159.
10. Fyfe CA, Brouwer DH, Lewis AR, Villaescusa LA, Morris RE (2002) Combined solid state NMR and X-ray diffraction investigation of the local structure of the five-coordinate silicon in fluoride-containing as-synthesized STF zeolite. *J Am Chem Soc* 124(26):7770–7778.
11. Villaescusa LA, Bull I, Wheatley PS, Lightfoot P, Morris RE (2003) The location of fluoride and organic guests in “as-made” pure silica zeolites FER and CHA. *J Mater Chem* 13(8):1978–1982.
12. George AR, Catlow CRA (1995) An investigation into the effects of ion incorporation on the electronic structure of silicate fragments via ab initio computational techniques. *Chem Phys Lett* 247(4-6):408–417.
13. George AR, Catlow CRA (1997) A computational study of the role of F ions in the octadecasil structure. *Zeolites* 18(1):67–70.
14. Park SS, et al. (2004) Endohedral and exohedral complexes of polyhedral double four-membered-ring (D4R) units with atomic and ionic impurities. *J Phys Chem A* 108(51):11260–11272.
15. Tossell JA (2007) Calculation of ¹⁹F and ²⁹Si NMR shifts and stabilities of F- encapsulating silsesquioxanes. *J Phys Chem C* 111(9):3584–3590.
16. Laine RM, Roll MF (2011) Polyhedral phenylsilsesquioxanes. *Macromolecules* 44(5):1073–1109.
17. Calzaferri G, Hoffmann R (1991) The symmetrical octasilsesquioxanes X8Si8O12: Electronic structure and reactivity. *J Chem Soc Dalton Trans* (5):917–928.
18. Auf der Heyde TPE, Bürgi HB, Bürgi H, Törnroos KW (1991) The crystal and molecular structure of the symmetrical silsesquioxane H₈Si₈O₁₂ at 100K, a molecular building block of some zeolites. *Chimia (Aarau)* 45(1-2):38–40.
19. Adarsh NN, Grélard A, Dufourc EJ, Dastidar P (2012) Sequestering hydrated fluoride in a three-dimensional non-interpenetrated octahedral coordination polymer via a single-crystal-to-single-crystal fashion. *Cryst Growth Des* 12(7):3369–3373.
20. Kalita ACh, Murugavel R (2014) Fluoride ion sensing and caging by a preformed molecular D4R zinc phosphate heterocubane. *Inorg Chem* 53(7):3345–3353.
21. Kang SO, Llinares JM, Powell D, VanderVelde D, Bowman-James K (2003) New polyamide cryptand for anion binding. *J Am Chem Soc* 125(34):10152–10153.
22. Kang SO, Llinares JM, Day VW, Bowman-James K (2010) Cryptand-like anion receptors. *Chem Soc Rev* 39(10):3980–4003.
23. Wang Q-Q, Day VW, Bowman-James K (2012) Supramolecular encapsulation of tetrahedrally hydrated guests in a tetrahedron host. *Angew Chem Int Ed Engl* 51(9):2119–2123.
24. Dey SK, Das G (2011) A selective fluoride encapsulated neutral tripodal receptor capsule: Solvatochromism and solvatomorphism. *Chem Commun (Camb)* 47(17):4983–4985.
25. Guchhait T, Mani G, Schulzke C, Anoop A (2012) A tripyrrolylmethane-based macrobicyclic triazacryptand: X-ray structure, size-selective anion binding, and fluoride-ion-mediated proton-deuterium exchange studies. *Inorg Chem* 51(21):11635–11644.
26. Fyfe CA, Brouwer DH, Lewis AR, Chézeau JM (2001) Location of the fluoride ion in tetrapropylammonium fluoride silicalite-1 determined by ¹H/¹⁹F/²⁹Si triple resonance CP, REDOR, and TEDOR NMR experiments. *J Am Chem Soc* 123(28):6882–6891.
27. Albright TA, Burdett JK, Whangbo MH (2013) *Orbital Interactions in Chemistry* (Wiley, New York), 2nd Ed, pp 15–32.
28. Grimme S, Antony J, Ehrlich S, Krieg H (2010) A consistent and accurate ab initio parametrization of density functional dispersion correction (DFT-D) for the 94 elements H-Pu. *J Chem Phys* 132(15):154104.
29. Ziegler T, Rauk A (1979) A theoretical study of the ethylene-metal bond in complexes between Cu⁺, Ag⁺, Au⁺, Pt⁰, or Pt²⁺ and ethylene, based on the Hartree-Fock-Slater transition-state method. *Inorg Chem* 18(6):1558–1565.
30. Fernández I, Bickelhaupt FM (2014) The activation strain model and molecular orbital theory: Understanding and designing chemical reactions. *Chem Soc Rev* 43(14):4953–4967.
31. Akiba K (1998) *Chemistry of Hypervalent Compounds* (Wiley, New York), p 5.
32. Pierrefixe SCAH, van Stralen SJM, van Stralen JNP, Fonseca Guerra C, Bickelhaupt FM (2009) Hypervalent carbon atom: “Freezing” the S_{(N)2} transition state. *Angew Chem Int Ed Engl* 48(35):6469–6471.
33. Mayer I (1983) Charge, bond order and valence in the AB initio SCF theory. *Chem Phys Lett* 97(3):270–274.
34. Braïda B, Hiberty PC (2013) The essential role of charge-shift bonding in hypervalent prototype XeF₂. *Nat Chem* 5(5):417–422.
35. Braïda B, Hiberty PC (2015) Erratum: The essential role of charge-shift bonding in hypervalent prototype XeF₂. *Nat Chem* 7(12):1033.
36. Braïda B, Ribeyre T, Hiberty PC (2014) A valence bond model for electron-rich hypervalent species: Application to SF_n (n=1, 2, 4), PF₅, and ClF₃. *Chemistry* 20(31):9643–9649.
37. Pierrefixe SCAH, Fonseca Guerra C, Bickelhaupt FM (2008) Hypervalent silicon versus carbon: Ball-in-a-box model. *Chemistry* 14(3):819–828.
38. Hiberty PC, Danovich D, Shurki A, Shaik S (1995) Why does benzene possess a D_{6h} symmetry? A quasiclassical state approach for probing π-bonding and delocalization energies. *J Am Chem Soc* 117(29):7760–7768.
39. Caultel P, Paillaud J-L, Simon-Masseron A, Soulard M, Patarin J (2005) The fluoride route: A strategy to crystalline porous materials. *Cr Chim* 8(3):245–266.
40. Liu X, Ravon U, Tuel A (2011) Fluoride removal from double four-membered ring (D4R) units in As-synthesized Ge-containing zeolites. *Chem Mater* 23(22):5052–5057.
41. Liu X, Ravon U, Bosselet F, Bergeret G, Tuel A (2012) Probing Ge distribution in zeolite frameworks by post-synthesis introduction of fluoride in as-made materials. *Chem Mater* 24(15):3016–3022.